Amelioration of Diabetic Nephropathy in SPARC-Null Mice

SEKIKO TANEDA,* JEFFREY W. PIPPIN,† E. HELENE SAGE,‡ KELLY L. HUDKINS,* YASUO TAKEUCHI,† WILLIAM G. COUSER,† and CHARLES E. ALPERS*

**Department of Pathology, †Division of Nephrology, University of Washington, Seattle Washington; and ‡Department of Vascular Biology, The Hope Heart Institute, Seattle, Washington.*

Abstract. SPARC (Secreted Protein, Acidic and Rich in Cysteine) is a matricellular protein that inhibits mesangial cell proliferation and also affects production of extracellular matrix (ECM) by regulating transforming growth factor-β1 (TGF-β1) and type I collagen in mesangial cells. This study is an investigation of the role of SPARC in streptozotocin (STZ)–induced diabetic nephropathy (DN) of 6-mo duration in wild type (WT) and SPARC-null mice. SPARC expression was evaluated by immunohistochemistry (IHC) and by *in situ* hybridization (ISH). Deposition of type I and IV collagen and laminin was evaluated by IHC, and TGF-β 1 mRNA was assessed by ISH. Renal function studies revealed no significant difference in BUN between diabetic SPARC-null mice and diabetic WT mice, whereas a significant increase in albumin excretion was detected in diabetic WT relative to diabetic SPARC-null mice. Diabetic WT animals exhibited increased levels of SPARC mRNA and protein in glomerular epithelial cells and in interstitial cells, in comparison with nondiabetic WT mice. Neither SPARC mRNA nor protein was detected in SPARC-null mice. Morphometry revealed a significant increase in the percentage of the glomerular tufts occupied by ECM in diabetic WT compared with nondiabetic WT mice, although there was no difference in the mean glomerular tuft area among groups. In contrast, diabetic SPARC-null mice did not show a significant difference in the percentage of the glomerular tufts occupied by ECM relative to nondiabetic null mice. Tubulointerstitial fibrosis was ameliorated in diabetic SPARC-null mice compared with diabetic WT animals. Further characterization of diabetic SPARC-null mice revealed diminished glomerular deposition of type IV collagen and laminin, and diminished interstitial deposition of type I and type IV collagen correlated with decreases in TGF-β 1 mRNA compared with WT diabetic mice. These observations suggest that SPARC contributes to glomerulosclerosis and tubulointerstitial damage in response to hyperglycemia through increasing TGF-β 1 expression in this model of chronic DN.

SPARC (Secreted Protein, Acidic and Rich in Cysteine, Osteonectin, BM-40, 43-kD protein) is a matricellular protein that does not function as a structural component of the extracellular matrix (ECM) but has important interactions with matrix proteins (1). The diversity of its biologic functions is exemplified by its ability to modulate the interactions between cells and ECM proteins such as collagen type I (2), inhibit cell proliferation and cell adhesion (3), interact with certain growth factors such as platelet-derived growth factor (PDGF) and vascular endothelial growth factor (VEGF) (4), and induce the expression of transforming growth factor-β1 (TGF-β1) in renal cells (5,6). *In vivo,* SPARC is expressed during development (7) and is detected at sites of wound repair (8) and tissue remodeling (9). SPARC has also been implicated in the progression of renal injuries. *In vivo,* increased production of SPARC mRNA is observed in visceral glomerular epithelial cells and in interstitial cells in the course of passive Heymann nephritis (10) and in mesangial cells in the course of the anti-Thy-1 mesangial proliferative glomerulonephritis (11). *In vitro,* it has been demonstrated that SPARC may be involved in glomerular diseases by inhibiting mesangial cell proliferation and also by promoting production of ECM through regulation of TGF-β1 expression and type I collagen production by mesangial cells (5,11).

Diabetic nephropathy (DN) is one of the major complications and causes of death in diabetes (12). Increased thickness of glomerular basement membrane and augmentation of ECM are recognized as pathologic hallmarks of diabetes. The latter particularly contributes to the reduction of filtration surface area, which becomes important in advanced DN. Increased synthesis of ECM components is associated with the accumulation of mesangial matrix in DN, which is, at least partially, a consequence of the activity of certain growth factors. Numerous growth factors have been implicated in the development of DN such as TGF-β, a potent stimulus for the production of ECM through its regulation of the synthesis of ECM components, *e.g.*, collagen type I (13,14).

A study in humans demonstrated that significantly elevated serum concentrations of SPARC could be detected in diabetic patients with fibrosing renal injury as revealed by renal biopsy

Received October 29, 2002. Accepted December 12, 2002.
Dr. Jared J. Grantham served as Guest Editor and supervised the review and final disposition of this manuscript.
Correspondence to Dr. Charles E. Alpers, University of Washington Medical Center, Department of Pathology, Box 356100, 1959 NE Pacific St., Seattle, WA 98195. Phone: 206-543-5616; Fax: 206-543-3644; E-mail: calp@u.washington.edu

1046-6673/1404-0968
Journal of the American Society of Nephrology

DOI: 10.1097/01.ASN.0000054498.83125.90

(15). In an experimental model of rat DN induced by streptozotocin (STZ), a reduction of SPARC is observed in the early phase of injury, which coincides with the onset of diabetes-related kidney growth (16). The role of SPARC in DN, especially in the chronic phase of the disease, has not been extensively investigated and remains obscure. Mice with a homozygous deletion of the Sparc gene allow us to examine the role of SPARC in the pathogenesis of various diseases (17). Therefore, we conducted this study in SPARC-null mice to test the hypothesis, suggested by the study in humans cited above (15), that the absence of SPARC would ameliorate chronic DN.

Materials and Methods

Animals

The procedures used were approved by the local Animal Care Committee of the University of Washington. The establishment of SPARC-null mice has been previously described (17). SPARC-null (−/−) mice and wild-type (WT) (+/+) mice were maintained in a pathogen-free facility, where all animals had free access to water and were fed the standard rodent chow composed of 24% of protein and less than 4% of fat (Harlan TEKLAD, Madison, WI). A mixed genetic background (F_2) of 129/SvJ × C57BL/6J wild-type (WT) (+/+) and SPARC-null (−/−) mice was used for this study.

Disease Model

Seven to ten-week-old male mice weighing 19 to 35 g at the onset of the experimental protocol were randomly divided into two groups: (*1*) a group in which mice were treated with STZ (Sigma Chemical Co., St. Louis, MO) and (*2*) a group in which mice were treated with citrate buffer adjusted to pH 4.5 (Sterile Water for Irrigation; Baxter Healthcare Corp., Deerfield, IL). STZ was dissolved in sterile citrate buffer and injected intraperitoneally into mice (120 mg/kg, up to 0. 4 ml) within 10 min of preparation. STZ or citrate buffer was administered at three time points occurring at 48-h intervals during the first week of this study.

Serum glucose levels and body weight were examined every 2 wk during the first 2 mo after injections and subsequently every 4 wk until sacrifice. Blood was collected from the orbital sinus.

Urinary glucose level was monitored semiquantitatively with Uristix reagent strips (Bayer Corporation, Elkhart, IN) every week during the first 2 mo according to the manufacturer's instructions. Grading for urinary glucose was as follows; 0 (negative), 1+ (>100 mg/dl), 2+ (>250 mg/dl), 3+ (>500 mg/dl), 4+ (>1000 mg/dl), or 5+ (>2000 mg/dl). To render animals hyperglycemic without becoming ketoacidotic, when the urinary glucose level of diabetic mice was more than 5+, we administered long-acting insulin (Humulin U, Ultralente, human insulin HI-610; Eli Lilly and Co., Indianapolis, IN) subcutaneously at a dose of 1 unit three times every 2 d. Serum glucose levels after insulin treatment of the mice remained above 200 mg/dl.

The genotype of each animal was confirmed by PCR analysis on purified spleen DNA that was obtained at sacrifice.

Experimental Design

Twenty mice treated with STZ (SPARC-null mice, $n = 13$; WT mice, $n = 7$) and 13 mice treated with citrate buffer alone (SPARC-null mice, $n = 7$; WT mice, $n = 6$) were sacrificed 6 mo after these injections. Six-hour urine samples were collected in each mouse one day before sacrifice. A blood sample was obtained via cardiac puncture at sacrifice. Kidneys were removed and rapidly processed for light microscopy, immunohistochemistry, and *in situ* hybridization using conventional fixatives and techniques. Spleens were taken for genotyping by PCR analysis and snap-frozen in isopentane.

Renal tissues from these mice were evaluated by immunohistochemistry for SPARC, α-smooth muscle actin (αSMA, a marker of activated mesangial cells or myofibroblastic interstitial cells), Ki-67 (a marker of proliferating cells), Mac-2 (a marker of monocytes/macrophages), type I collagen (component of ECM) and type IV collagen, and laminin (components of the basement membrane). Expression of SPARC mRNA and TGF-β 1 mRNA was evaluated by *in situ* hybridization.

Preparation of DNA and Genotyping

The Dneasy Tissue Kit (Qiagen Inc.) was used for DNA isolation from the spleens (up to 10 mg) according to the protocol of the manufacturer.

Mice were genotyped using three PCR primers as described previously (Life Technologies BRL, Rockville, MD) (18): 5'GATGAGGGTGGTCTGGCCCAGCCCTAGATGCCCCTCAC3', from the 5' end of the coding region of the SPARC gene; 5'CACCCACACAGCTGGGGGTGATCCAGATAAGCCAAG3', from the 3' end of the coding region, and 5'GTTGTGCCCAGTCATAGCCGAATAGCCTCTCCACCCAAG3', which was annealed with a sequence within the neomycin insertion region. A DNA product of 300 bp was demonstrated in WT animals, and one of 550 bp was demonstrated in SPARC-null mice. The DNA product isolated from heterozygotes was characterized by the presence of both bands. The PCR reaction contained DNA, 10 × PCR buffer, 50 mM $MgCl_2$, 12.5 μM of each primer, 10 mM dNTP (Life Technologies BRL), and 2.5 units of *Taq* DNA polymerase (MBI Fermentas, Hanover, MD) in a 50-μl PCR reaction. Cycling conditions were: 96°C for 1 min, followed by 40 cycles at 96°C for 30 s, 60°C for 45 s, 68°C for 4 min, and 74°C for 10 min.

Renal Morphology

Renal tissue was divided and fixed in either 10% neutral-buffered formalin or in methyl Carnoy solution, as described previously (19). Fixed tissues were processed, embedded in paraffin according to standard protocols, and sectioned at 4 μm. Slides were stained with periodic acid methenamine silver (silver), with periodic acid-Schiff (PAS), and with hematoxylin and eosin (H&E) using standard histologic procedures. Semiquantitative scoring of glomerular sclerosis in silver-stained tissue utilized five grades as described previously (20): 0 = normal glomerulus, 1+ = sclerosis involving less than 25% of glomerular surface area, 2+ = sclerosis involving 25 to 50%, 3+ = 50 to 75%, and 4+ = sclerosis involving 75% to 100% of glomerular surface area. Tubulointerstitial damage was also graded in the areas where 100 glomeruli were counted as described previously (21): 0 = no lesions showing cell infiltration and fibrosis, 1+ = minimal injury (single focus of lesion), 2+ = mild injury (more than two isolated foci), 3+ = moderate injury (more than five isolated foci), and 4+ = severe injury (more than ten isolated foci or diffuse infiltration and fibrosis).

Immunohistochemistry

Four-micrometer sections of formalin- and methyl Carnoy-fixed, paraffin-embedded tissue were processed by an indirect immunoperoxidase technique as described previously (19,22). The antibodies used in this study are listed in Table 1. Rabbit anti-mouse SPARC IgG from antiserum 5944 was affinity-purified as described previously (23). This polyclonal preparation immunoprecipitated SPARC from

Table 1. Antibodies used to detect specific antigens in biopsy tissue[a]

Antigen	Clone	Primary Antibody	Dilution of Primary Antibody	Reference
K_i-67	B56	Mouse IgG1 monoclonal antibody anti-human K_i-67 (BD Biosciences, San Diego, CA)	1:100	41
α-Smooth muscle actin	1A4	Mouse monoclonal IgG2a anti-human α-smooth muscle actin (DAKO)	1:25	42
Type I collagen		Goat polyclonal antibody anti-human collagen I (Southern Biotechnology, Birmingham, AL)	1:1000	43
Type IV collagen		Goat polyclonal antibody anti-human collagen IV (Southern Biotechnology)	1:600	44
Laminin		Rabbit polyclonal antibody anti-rat laminin (Chemicon, Temecula, CA)	1:7000	45
SPARC		Rabbit polyclonal antibody anti-mouse SPARC (5944)	1:800	23
Mac-2	M3/38	Rat IgG monoclonal antibody anti-mouse Mac-2 (CEDARLANE, Hornby, Ontario, Canada)	1:5000	46

[a] All antigens were detected in methyl Carnoy-fixed tissue, except for Mac-2, which was detected in formalin-fixed tissue. Laminin was digested with Protease type XXIV (Sigma). K_i-67 was used with the DAKO animal research kit to allow detection of a primary murine antibody in murine tissues.

the conditioned media of murine glomerular mesangial cells, but did not react with any protein from the conditioned media of mesangial cells from SPARC-null mice (18). The specificity of the other antibodies has been established as referenced. For all samples, negative controls for the immunohistochemistry included substitution of the primary antibody with an irrelevant IgG from the same species or with phosphate-buffered saline (PBS).

All slides were scored by an observer blinded to the origin of the histologic specimen. Semiquantitative scoring of glomerular expression of αSMA, types I and IV collagen, and laminin was performed using five grades as follows: 0 = no staining; 1+ = mesangial staining involving less than 25% of the area examined; 2+ = segmental mesangial staining involving 25 to 50% of mesangial areas present; 3+ = mesangial staining involving 50 to 75% of the areas examined; 4+ = diffuse mesangial staining involving more than 75% of areas examined, as described previously (19). The number of Mac-2-expressing cells and of Ki-67-positive cells in the glomerular tufts was identified by immunostaining and counted at a magnification of $\times$400. Both the number of the intraglomerular positive cells and the number of glomeruli were counted, and the data are presented as stained cells per glomerular cross-section (gcs). Cells outside the glomerular tufts were excluded from these counts. At least 20 consecutive cross-sections of glomeruli (counting only those glomeruli containing more than 20 discrete capillary segments) were examined with each of the above antibodies. The degree of tubulointerstitial changes was graded on a scale from 0 to 4 as follows: 0 = normal kidney; 1+ = minimal abnormalities affecting less than 25% of the renal parenchyma; 2+ = mild, 25 to 50% involvement; and 3+ = moderate, 50 to 75% involvement, 4+ = severe, more than 75% of the kidney manifesting abnormalities.

Urine and Blood Samples

Serum glucose levels and semiquantitative urinary glucose levels at sacrifice were examined as mentioned above using the Genuine One Touch and One Touch Basic (Lifescan Inc., Milpitas, CA) and with Uristix reagent stripes (Bayer Corporation), respectively. Blood urea nitrogen (BUN) was determined by a commercial colormetric assay (Sigma). Urine samples were evaluated for proteinuria using the albumin/creatinine ratio. Albuminuria was evaluated using the Albuwell (Exocell, Inc., Philadelphia, PA) mouse albumin ELISA, and creatinine was measured using The Creatinine Companion (Exocell) according to the protocols of the manufacturer.

Molecular Probes

The molecular probes used in this study have previously been described (24,25):

1. SPARC: a 427-bp fragment of the human cDNA was inserted into a pGEM-T Vector (Promega, Madison, WI).
2. TGF-β1: a 974-kb (nt 421 to 1395) fragment of the mouse cDNA was inserted into the *Sma*I site of pGem7Zf+ (Promega), and was a gift from H.L. Moses, Dept. Cell Biology, Vanderbilt University, Nashville, TN (26).

Both antisense and sense riboprobes were transcribed using reagents from Promega, except [^{35}S]-UTP, which was obtained from New England Nuclear (Boston, MA). The details of this procedure have been published (27).

In Situ Hybridization

The *in situ* hybridization protocols have been described in detail (27). Negative controls included hybridization performed on replicate tissue sections using the sense riboprobe.

The extent of intraglomerular hybridization signal was graded semiquantitatively by an observer who was blinded to the origin of the histologic specimen: 0 = absent, 1 = mild (a few positive cells), 2 = moderate (several positive cells in a segmental distribution within the glomerulus), 3 = severe (many positive cells in a diffuse distribution).

Morphometric Analyses

Morphometric analysis was performed on H&E-stained and silver-stained histologic sections as described previously (22). In a blinded fashion, 15 consecutive glomerular cross-sections were photographed with a digital camera (Olympus DP11, Olympus America Inc.,

Melville, NY) and imported into Image-Pro Plus (Media Cybernetics, Silver Spring, MD). The following parameters were measured for each glomerular cross-section: (*1*) The number of glomerular nuclei and the glomerular tuft area (independent of the urinary space) on H&E-stained tissue and (*2*) the area of mesangial matrix and the glomerular tuft area on silver-stained tissue.

Statistical Analyses

All values are expressed as the mean ± SEM. Using the SPSS program, version 10.0 for Windows (SPSS Inc. Chicago, IL), we determined the survival rate by Kaplan-Meier test. Urinary glucose was compared by a nonparametric Mann-Whitney *U* test. Other data were examined with one-way ANOVA following Tukey post-hoc test. A $P < 0.05$ was considered to be statistically significant.

Results

Survival Rate

Diabetes was induced by STZ injections in 29 mice, 17 from SPARC-null mice and 12 from WT mice, at the beginning of this study. Two SPARC-null mice and one WT mouse received insulin injections subcutaneously during the first 2 wk. Seven mice died (three SPARC-null mice and four WT mice) during the initial 6 wk of observation, including the three mice that received insulin injections. Uncontrolled severe hyperglycemia and consequent dehydration were the presumed causes of death of these mice. Two additional mice died during the remaining course of the study, one SPARC-null mouse after 14 wk, and one WT mouse after 20 wk of observation. Blood, urine, and renal tissue specimens could not be collected from these animals. Twenty animals (13 SPARC-null mice and 7 WT mice) survived for the entire 24-wk study. The survival rate of diabetic animals through the entire 24-wk observation period was 13 of 17 for SPARC-null mice and 7 of 12 for WT mice, a difference without statistical significance ($P = 0.33$).

Metabolic Characteristics and Renal Function

Metabolic parameters, body weight, and serum glucose level are presented in Table 2. The body weight of diabetic groups reached a nadir at 2 wk and gradually increased thereafter. Nondiabetic groups had a significant body weight gain compared with diabetic groups after 12 wk and at the end of the study period.

Both diabetic groups had significantly elevated blood glucose levels compared with the nondiabetic groups throughout the 24-wk observation period. There was no significant difference in blood glucose levels between diabetic SPARC-null and WT mice.

Renal function as measured by BUN revealed that diabetic groups of both genotypes showed a significant increase in BUN compared to nondiabetic groups (Table 2). However, no significant difference in BUN was detected between diabetic groups. Diabetic groups of both genotypes exhibited increases in albumin excretion, with an increased albumin/creatinine ratio compared with nondiabetic groups (Table 2). The albumin excretion of diabetic WT mice was significantly higher than that of diabetic SPARC-null mice. Diabetic groups of both genotypes had significant increases in both urinary glucose and urine volume, but there were no significant differences between the genotypes for these parameters (Table 2).

SPARC-Null Mice Show Reduced Accumulation of ECM

No segmental or global glomerulosclerosis was observed in renal tissue specimens obtained from nondiabetic WT or SPARC-null mice (Figure 1, B and E). Diabetic WT mice manifested extensive mesangial matrix expansion (Figure 1H), whereas no apparent increase of mesangial matrix was observed in diabetic SPARC-null mice (Figure 1K). No significant increase in glomerular cell number was noted in diabetic

Table 2. Variables measured during the study period of STZ-diabetes

	WT Mice with Citrate Buffer	WT Mice with STZ	SPARC-Null Mice with Citrate Buffer	SPARC-Null Mice with STZ
Body weight (g)				
initial	25.6 ± 0.8	30.9 ± 2.3	23.3 ± 0.5	24.8 ± 0.9
2 wk	25.3 ± 0.6[d]	26.6 ± 2.1	22.8 ± 0.3	23.5 ± 1.0
12 wk	35.0 ± 0.9[c]	29.2 ± 1.3[ac]	28.2 ± 0.9	25.1 ± 0.6[a]
24 wk	40.1 ± 1.7	29.6 ± 1.9[b]	31.3 ± 1.2	26.0 ± 0.9[b]
Serum glucose (mg/dl)				
initial	107.2 ± 6.1[c]	118.7 ± 7.8	117.9 ± 6.6	122.7 ± 3.3
2 wk	107.0 ± 8.5[d]	278.2 ± 22.5[b]	122.1 ± 3.4	265.0 ± 10.3[b]
12 wk	101.8 ± 4.7	348.3 ± 23.1[b]	97.6 ± 2.0	319.0 ± 22.2[b]
24 wk	150.6 ± 6.1	305.6 ± 21.4[b]	155.1 ± 17.1	367.9 ± 32.0[b]
Blood urea nitrogen (BUN) (mg/dl)	15.5 ± 1.7	35.9 ± 2.7[b]	14.1 ± 1.8	29.3 ± 2.7[b]
Urinary-μg Albumin/mg creatinine	41.1 ± 5.3	249.1 ± 37.9[bc]	43.5 ± 3.9	178.8 ± 13.3[b]
Urinary glucose	0	3.8 ± 0.4[b]	0	3.5 ± 0.3[b]
Urine volume (μl/6 h)	278.3 ± 80.3	690.0 ± 117.7[a]	171.4 ± 35.3	809.0 ± 103.3[b]

[a] $P < 0.05$, [b] $P < 0.01$ *versus* mice of the same genotype with citrate buffer injection.
[c] $P < 0.05$, [d] $P < 0.01$ *versus* SPARC-null mice receiving the same treatment.

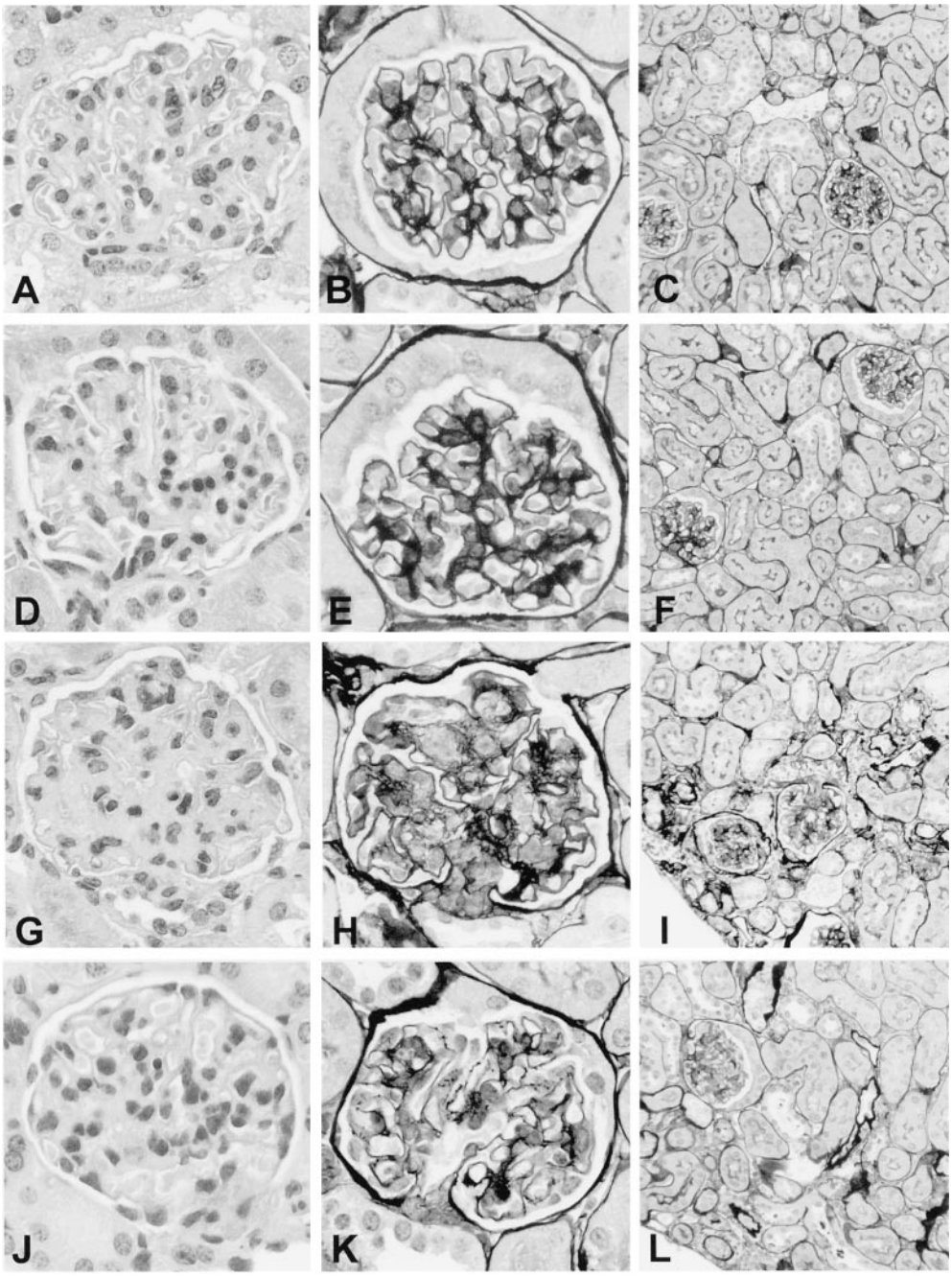

Figure 1. Light microscopic features of the glomerular lesions. Representative glomerulus and tubulointerstitium of a WT mouse (A, B, C) and SPARC-null mouse (D, E, F) treated with citrate buffer, stained with H&E (A and D), and silver methenamine (B, C, E, F). Representative glomerulus and tubulointerstitium of a WT mouse (G, H, I) and SPARC-null mouse (J, K, L) treated with STZ, stained with H&E (G and J), and silver methenamine (H, I, K, L). Widened mesangial areas are apparent in panels H and I only. Focal cellular infiltration and fibrosis involving the interstitium are frequently observed in I and to a lesser extent in L. No apparent change in glomerular cell number was detected in any of the groups studied. Original magnifications: ×200 in C, F, I, and L; ×400 in all others.

mice compared with nondiabetic mice (Figure 1, A, D, G, and J). The results of the semiquantitative analysis are summarized in Table 3. There was no significant difference in the scoring of glomerulosclerosis in silver-stained tissue between diabetic and nondiabetic SPARC-null mice by semiquantitative grading methods (see Materials and Methods). In contrast, diabetic WT mice showed a significant increase in the scoring of glomerulosclerosis compared with nondiabetic WT mice (diabetic 1.12 $\pm$ 0. 12 *versus* nondiabetic 0.26 $\pm$ 0. 02; $P < 0.01$), which was also significantly elevated compared with diabetic SPARC-null mice (WT 1.12 $\pm$ 0. 12 *versus* SPARC-null 0. 53 $\pm$ 0. 05; $P < 0.01$). In addition to the semiquantitative analysis, a quantitative analysis using morphometry was performed for the glomerular tuft area, glomerular matrix area, and glomerular

Table 3. Semiquantitative analysis of histopathology: mesangial expansion and tubulointerstitial injury

	Treatment	n[a]	Glomerular Sclerosis[d]	Tubulointerstitial Injury				
				0	1+	2+	3+	4+
WT	Citrate	6	0.26 ± 0.02	6	0	0	0	0
	STZ	7	1.12 ± 0.12[bc]	0	1	1	2	3
SPARC-null	Citrate	7	0.41 ± 0.07	7	0	0	0	0
	STZ	13	0.53 ± 0.05	2	7	3	1	0

[a] Total number of mice.
[b] $P < 0.01$ *versus* mice of the same genotype with citrate buffer injection.
[c] $P < 0.01$ *versus* SPARC-null mice receiving the same treatment.
[d] Glomerular sclerosis was semiquantitatively scored in silver-stained tissue from 0 to 4 determined by percent of sclerosis of glomerular surface area.

cellularity (Figure 2). By this approach, there was no difference in the size of glomerular tuft among the four groups (Figure 2A). There were also no significant differences in mean cell number per glomerular tuft area among the four groups (Figure 2, B and C). In silver-stained histologic sections, diabetic WT mice demonstrated a significant increase in the area occupied by matrix per glomerulus, in comparison with nondiabetic WT mice (Figure 2D). In contrast, diabetic SPARC-null mice did not show a significant difference compared with nondiabetic null mice (Figure 2D). The same was true for the percentage of matrix per tuft area (Figure 2E).

Tubulointerstitial lesions including focal leukocyte infiltration of the interstitium, fibrosis, and tubular dilatation and atrophy, were frequently observed in diabetic WT mice compared with diabetic SPARC-null mice (Figure 1, I and L; Table 3). No histologic changes in the vasculature were observed in any of the four groups.

Reduced Glomerular Accumulation of ECM Is Characterized by Type IV Collagen and Laminin Deposition in SPARC-Null Mice

To assess the specific composition of the ECM, we performed immunohistochemical staining for type I collagen, type IV collagen, and laminin. Nondiabetic mice of both genotypes demonstrated immunostaining for type IV collagen in the glomerular and tubular basement membranes. Glomerular staining for type IV collagen in nondiabetic mice was focal in distribution (Figure 3, B and E). A similar staining pattern for laminin was observed in nondiabetic kidneys of both genotypes (Figure 3, A and D). Diabetic WT mice demonstrated a significant increase in immunostaining for type IV collagen predominantly localized to the mesangium (Figure 3H; Table 4). Diabetic WT mice showed increased accumulation of laminin in both mesangium and glomerular capillary walls, in comparison with nondiabetic WT mice (Figure 3G; Table 4). In contrast, immunostaining for type IV collagen and laminin in diabetic SPARC-null mice compared with nondiabetic null mice was less (Figure 3, J and K; Table 4). In diabetic WT mice, deposition of type IV collagen and, to a lesser extent, of laminin was increased at sites of tubulointerstitial fibrosis compared with diabetic null mice (Figure 3, G, H, J, and K). Glomerular staining for type I collagen was consistently negative in both SPARC-null and WT mice (Figure 3, C, F, I, and L), but increased interstitial staining of this collagen was noted in both diabetic mice and was significantly enhanced in diabetic WT compared with diabetic null animals (Figure 3, I and L; Table 4).

Diabetic WT Mice Exhibit Increased Levels of SPARC mRNA and Protein

In nondiabetic WT mice, immunostaining revealed uniform expression of SPARC within the cytoplasm of visceral glomerular epithelial cells but no expression within the tubulointerstitium (Figure 4A). In contrast, in diabetic WT mice, SPARC expression appeared increased within the glomerular epithelial cells, but with occasional *de novo* expression by parietal epithelial cells (Figure 4, B and C). SPARC protein was not detected in mesangial cells. Immunostaining for SPARC was detected in the interstitial cells in association with areas of tubulointerstitial injury, but not within tubular epithelial cells in the diabetic mice (Figure 4D). No immunostaining for SPARC was observed in renal tissue obtained from SPARC-null mice (data not shown).

In situ hybridization using a SPARC antisense riboprobe revealed that SPARC mRNA and protein were essentially coincident. In nondiabetic WT mice, only a weak signal was present in glomeruli (Figure 4E). In contrast, diabetic WT glomeruli showed a significant increase in levels of SPARC mRNA (diabetic 2.7 ± 0.2 *versus* nondiabetic 1.3 ± 0.2; $P < 0.01$), which appeared to localize to visceral epithelial cells within the glomerular tufts (Figure 4F). In addition, diabetic WT mice exhibited *de novo* expression of SPARC mRNA in some parietal epithelial cells (Figure 4G) and increased SPARC mRNA in areas of tubulointerstitial injury (Figure 4H). SPARC mRNA was not detected in the interstitium of non-diabetic WT mice (Figure 4E). SPARC mRNA was not detected either in nondiabetic or diabetic SPARC-null mice (data not shown). Minimal background accumulation of silver grains was present on the tissue exposed to the sense probe control (data not shown).

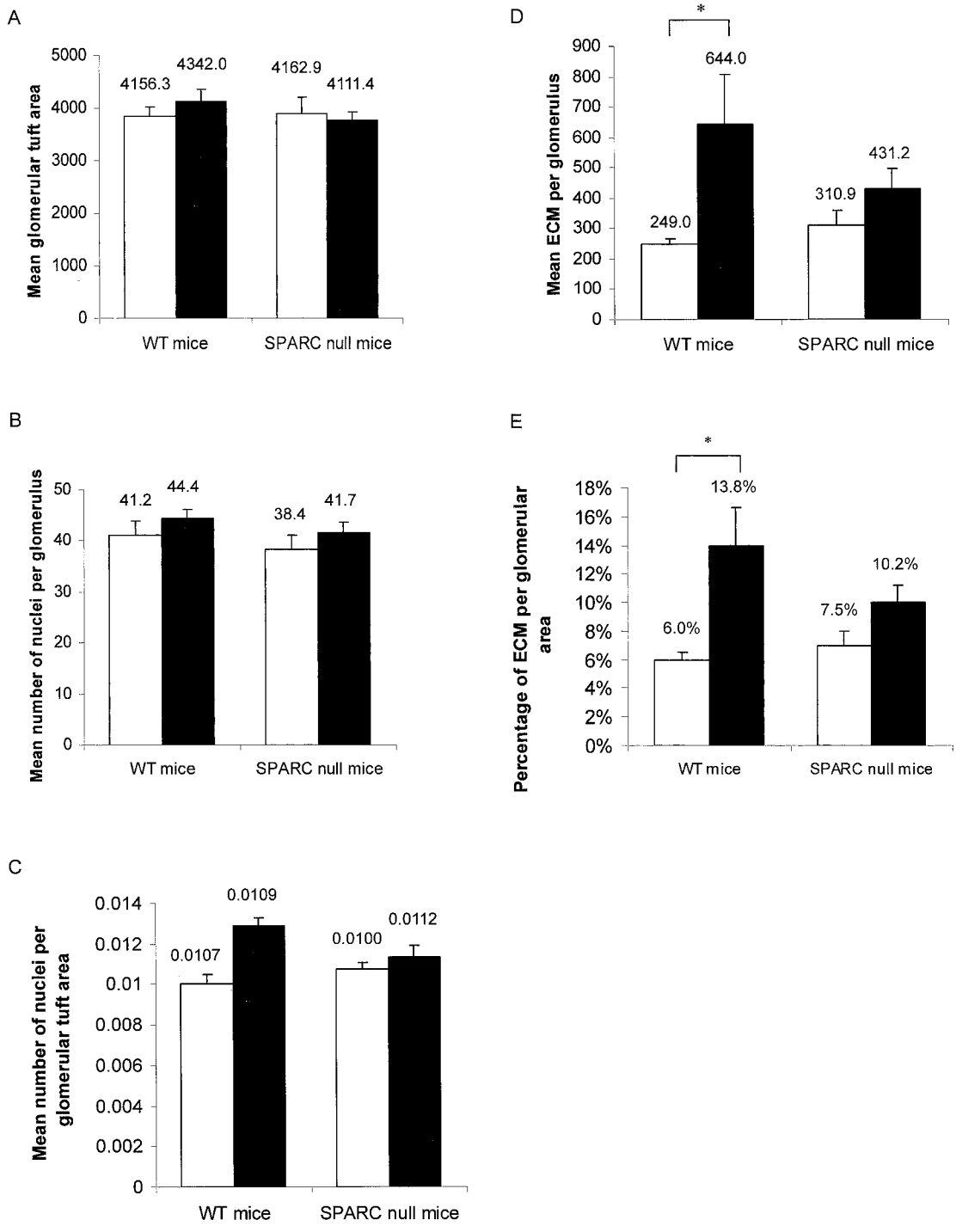

Figure 2. (A) Mean glomerular tuft area (μm^2), (B) mean cell number per glomerulus, (C) mean cell number per μm^2 of glomerular tuft area, (D) mean area of ECM per glomerulus (μm^2), (E) and percentage of ECM per glomerular tuft area in WT and SPARC null-mice with citrate buffer treatment (blank bar) and STZ treatment (black bar). Bars represent SEM; *$P < 0.05$.

Slight Elevation of αSMA Is Apparent in Diabetic WT and SPARC-Null Mice

We asked whether a phenotypic change of mesangial cells or interstitial cells occurs in this model of experimental diabetes. Accordingly, tissue was stained for the mesangial activation marker αSMA. All renal specimens obtained from SPARC-null and WT mice demonstrated intense staining for αSMA by the smooth muscle cells of muscular arteries. A few glomeruli in nondiabetic mice exhibited mesangial αSMA, usually in a segmental distribution within the glomerular tuft. No difference in αSMA expression was noted between diabetic and nondiabetic SPARC-null mice, whereas diabetic WT mice showed a slight elevation of αSMA in comparison with nondiabetic WT mice and diabetic SPARC-null mice (Table 4).

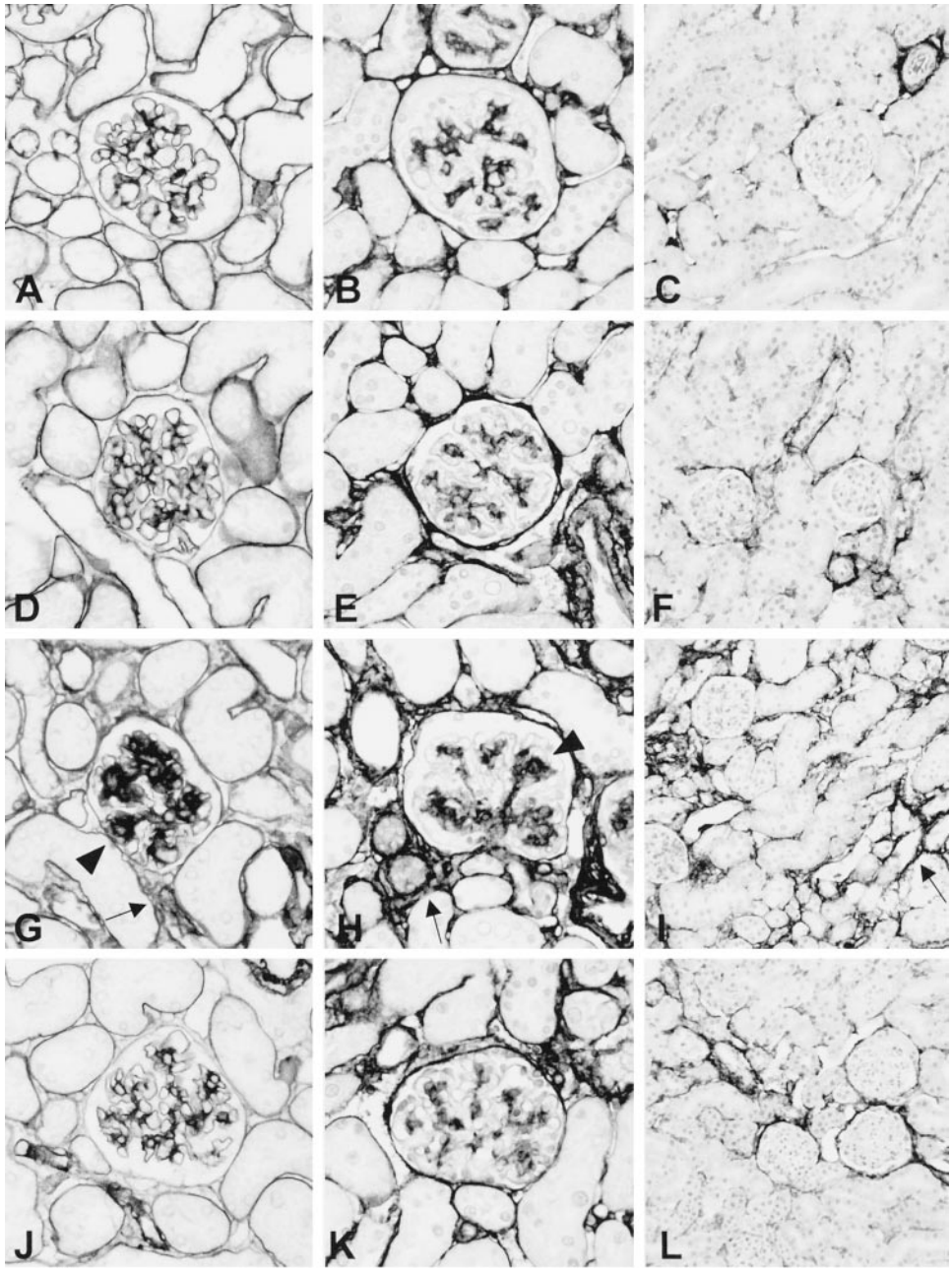

Figure 3. Immunohistochemical staining for ECM components. Immunohistochemistry for laminin (A, D, G, J), type IV collagen (B, E, H, K), and type I collagen (C, F, I, L) in a citrate buffer–treated WT mice (A through C) and SPARC-null mice (D through F) and STZ-treated WT mice (G through I) and null mice (J through L). Diabetic WT mice demonstrate an increase in collagen IV and laminin in a mesangial pattern (arrowheads) that is not present in the SPARC-null mice. Deposition of type IV and type I collagens, and to a lesser extent laminin, was increased in the interstitium of diabetic WT mice (arrows). Original magnifications: ×200 in C, F, I, and L; ×400 in all others.

Slight increases in αSMA staining were also observed in the interstitial cells obtained from the diabetic groups, but there were no apparent differences between genotypes (Table 4). αSMA was not expressed by tubular epithelium.

The mean number of proliferating cells in glomeruli as determined by Ki-67, and the mean number of monocytes/macrophages in glomeruli labeled with Mac-2, showed no significant differences between groups (Table 4).

Decreased Expression of TGF-β 1 mRNA in SPARC-Null Mice

Weak expression of TGF-β1 mRNA was detected in a pattern consistent with mesangial cell expression in nondiabetic mice of both genotypes, without clear differences (Figure 5, A and B). Diabetic WT mice showed a significant increase in glomerular expression of TGF-β 1 mRNA, relative to nondiabetic WT mice (nondiabetic 1.3 ± 0.3 *versus* diabetic 2.5 ±

Table 4. Immunohistochemical analyses of STZ-diabetes in WT and SPARC-null mice[a]

	WT Mice with Citrate Buffer	WT Mice with STZ	SPARC-Null Mice with Citrate Buffer	SPARC-Null Mice with STZ
K_i-67 positive (cells/gcs)	0.6 ± 0.1	0.7 ± 0.2	0.4 ± 0.1	0.5 ± 0.1
Mac-2 positive (cells/gcs)	0.8 ± 0.2	1.6 ± 0.4	0.7 ± 0.1	1.1 ± 0.2
αSMA				
glom	0.07 ± 0.03	0.32 ± 0.09[bd]	0.10 ± 0.04	0.13 ± 0.02
int	0.2 ± 0.2	0.8 ± 0.3[b]	0.1 ± 0.1	0.7 ± 0.2[b]
Collagen IV				
glom	1.8 ± 0.02	2.4 ± 0.1[c]	1.7 ± 0.2	2.2 ± 0.1
int	0.0 ± 0.0	2.8 ± 0.3[ce]	0.0 ± 0.0	1.8 ± 0.3[c]
Laminin				
glom	1.3 ± 0.1	2.1 ± 0.1[cd]	1.3 ± 0.1	1.6 ± 0.1
int	0.0 ± 0.0	2.3 ± 0.3[c]	0.0 ± 0.0	1.6 ± 0.1[c]
Collagen I				
glom	–	–	–	–
int	0.3 ± 0.2	2.9 ± 0.3[ce]	0.3 ± 0.2	1.7 ± 0.2[c]

[a] gcs, glomerular cross section; glom, glomerular; int, interstitial. Glomerular expression of αSMA, types I and IV collagen, and laminin was semiquantitatively scored using five grades from 0 to 4 determined by percent of mesangial staining of the mesangial area examined. The degree of tubulointerstitial changes was graded on a scale from 0 to 4 determined by percent of affected area of the renal parenchyma.
[b] $P < 0.05$, [c] $P < 0.01$ *versus* mice of the same genotype with citrate buffer injection.
[d] $P < 0.05$, [e] $P < 0.01$ *versus* SPARC-null mice receiving the same treatment.

0.2; $P < 0.01$; Figure 5, A and C). There was no significant difference in glomerular TGF-β1 mRNA between diabetic SPARC-null mice and nondiabetic null mice, although there was a trend toward increased production in the former groups (nondiabetic 1.4 ± 0.3 *versus* diabetic 1.9 ± 0.2; $P = 0.09$; Figure 5, B and D). The intensity of TGF-β1 mRNA was substantially decreased in diabetic SPARC-null compared with diabetic WT mice, but the difference between these two groups did not reach significance (WT 2.5 ± 0.2 *versus* null 1.9 ± 0.2; $P = 0.054$).

TGF-β1 mRNA was barely detectable in the interstitium of nondiabetic mice (Figure 5, A and B), whereas in diabetic mice, especially WT, TGF-β1 mRNA was markedly augmented in areas of tubulointerstitial injury (Figure 5, C and D).

Discussion

There are a number of features of the matricellular protein SPARC that indicate it could play an important role in the pathogenesis and evolution of diabetic nephropathy. These include its ability to induce synthesis of TGF-β1 by mesangial cells, leading to production of ECM components (5), its localization in myofibroblast-like interstitial cells in humans in settings of interstitial fibrosis (24), a report of increased circulating levels of SPARC in diabetic patients with fibrosing renal injury (15), and evidence that SPARC participates in early events of diabetic nephropathy as revealed in STZ-induced diabetes in the rat (16). This study used genetically modified mice deficient in SPARC as one approach to test the importance of SPARC in mediating a well-characterized model of experimental DN. Two principal findings emerged from this study: (*1*) in the absence of SPARC, the severity of DN is markedly diminished; (*2*) the absence of SPARC was correlated with the suppression of the normally increased production of TGF-β1 that occurs in this model, indicating one mechanism for the diminished accumulation of ECM that is observed in diabetic SPARC-null mice.

In this study, increased production of SPARC mRNA and protein was detected in diabetic WT mice compared with nondiabetic WT mice. In both diabetic and nondiabetic WT mice, SPARC expression in glomeruli was detected only in podocytes. This pattern of expression by podocytes is consistent with previous reports in rats (10,28,29) and humans (24), although it has been reported under some disease conditions that mesangial cells produce SPARC as well (11,28). Mesangial production of SPARC was not detected in this study. Increased expression of SPARC in diabetic WT mice compared with nondiabetic WT mice was also detected in interstitial cells in areas of interstitial injury. This result is also consistent with data on renal interstitial fibrosis in rats (29) and humans (30).

The WT diabetic animals developed the characteristic features of STZ-induced DN as previously established: mesangial matrix expansion in the glomeruli, tubulointerstitial injury, and an absence of vascular pathology (31). The reduced severity of DN in SPARC-null compared with WT mice was defined by the following features: (*1*) reduction of mesangial matrix expansion with diminished accumulation of type IV collagen and laminin and (*2*) decreased interstitial injury with diminished deposition of type IV and type I collagen in the tubulointerstitium. A functional correlate to this morphologic improvement was a significant decrease in albumin excretion in the diabetic SPARC-null mice as compared with diabetic WT mice. These results are particularly relevant to human DN, which is characterized by increased expression of type IV collagen and

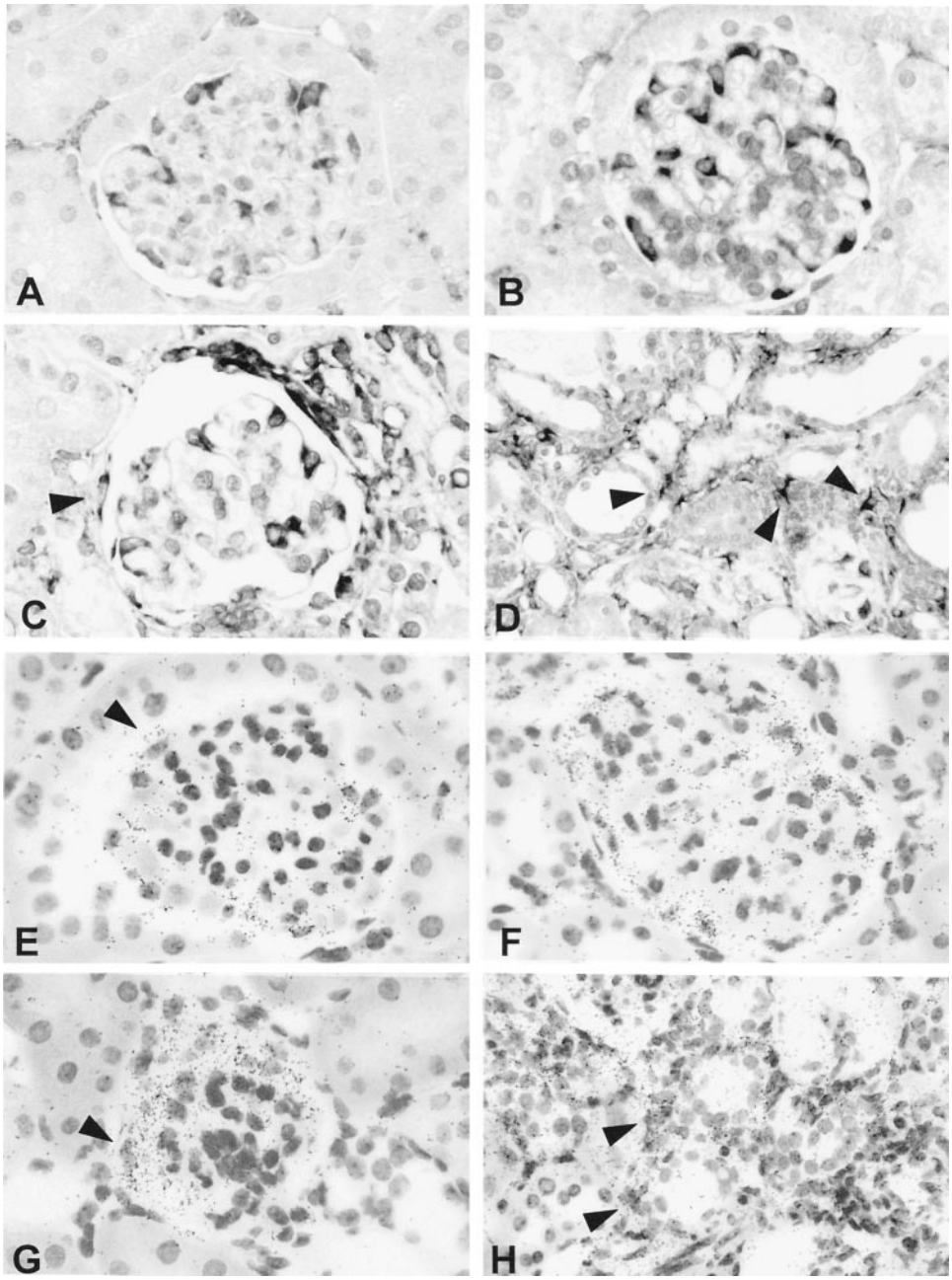

Figure 4. Expression of SPARC protein and mRNA. Immunostaining for SPARC in nondiabetic WT mice (A), and diabetic WT mice (B through D). (A and B) SPARC protein was uniformly expressed by visceral glomerular epithelial cells. (C) SPARC protein in parietal epithelial cells was occasionally detected (arrowhead). (D) Increased SPARC immunostaining was detected in interstitial cells in area of tubulointerstitial damage (arrowheads). *In situ* hybridization using a SPARC antisense riboprobe (E through H) performed on tissue sections from WT mice (E, citrate buffer–treated mice; F through H, STZ-treated mice). (E) Hybridization signal is concentrated in glomerular epithelial cells (arrow), with essentially the same distribution seen in panel A. (F) Diabetic WT mice showed significant increases in the glomerular expression of SPARC mRNA compared with nondiabetic mice. (G) Increased expression of SPARC mRNA by parietal epithelial cells was observed (arrowhead). (H) Increased expression of SPARC mRNA by in interstitial cells was detected in areas of interstitial damage (arrowheads). Original magnification, ×400.

laminin in the glomerular mesangial areas and in the peripheral capillary walls (32,33).

We speculate the beneficial effect of the SPARC deletion in diabetic nephropathy may be indirect, given that glomerular SPARC expression was identified in podocytes rather than mesangial cells, where the principal injury of experimental DN is localized. We speculate SPARC is active in part through physicochemical interactions with specific growth factors, such as that reported with PDGF B-chain (4), or may act to modify production of matrix regulatory molecules, such as

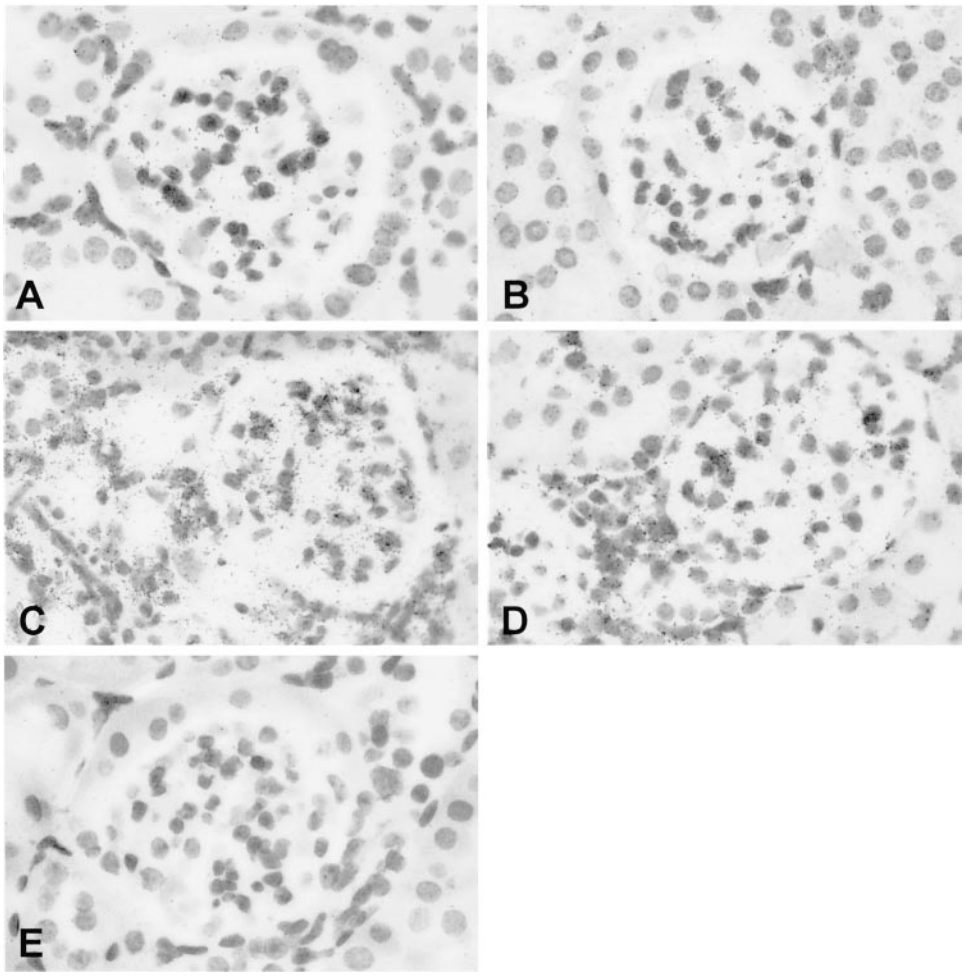

Figure 5. In situ hybridization for TGF-β1 mRNA. *In situ* hybridization using a TGF-β1 antisense riboprobe (A through D) and a sense riboprobe control (E) performed on tissue sections from citrate buffer-treated mice (A, WT; B, SPARC-null) and STZ-treated mice (C, WT; D, SPARC-null). Only a weak signal was present in nondiabetic mice, whereas diabetic groups showed an increase in glomerular expression of TGF-β 1 mRNA, most prominently in the WT mice. Diabetic WT mice also demonstrated an increased expression of TGF-β 1 mRNA in areas of tubulointerstitial injury that was not present in SPARC-null mice. Minimal background accumulation of silver grains is present in panel E. Original magnification, $\times$400.

TGF-β, which may be produced and released by glomerular epithelial cells in certain disease settings.

It is well established that TGF-β1 is a potent stimulator of ECM production in glomerular injury and may be the most important growth factor in determining the extent of renal fibrosis after injury. In the present study, we observed significant augmentation of TGF-β1 mRNA production as well as marked accumulation of glomerular ECM in diabetic WT mice compared with nondiabetic WT mice, consistent with previous studies in animal model systems of diabetes (34–36) and in human DN (35). A key finding of this study was that diabetic SPARC-null mice demonstrated suppression of the typical increases in TGF-β1 mRNA that occur in this model. It has been shown that TGF-β mediates the production of type I and type IV collagens in mesangial cells under conditions of high glucose *in vitro* (37). Exposure of cultured glomerular epithelial cells to TGF-β1 and high glucose concentrations also increased the production of the basement membrane components, laminin and type IV collagen (38). It was previously demonstrated that SPARC-null mesangial cells express significantly decreased steady-state levels of TGF-β1 mRNA and correspondingly less secreted TGF-β1 protein (5). We now demonstrate the relevance of this observation to the *in vivo* setting, where the absence of SPARC resulted in decreased synthesis of TGF-β 1 mRNA by mesangial cells, which presumably led to the reduced accumulation of ECM in glomeruli and basement membrane. These findings indicate SPARC can be an important mediator of sclerosing glomerular injury and acts at least in part by its ability to enhance TGF-β 1 expression.

In addition to the glomeruli, TGF-β1 expression was substantially increased in diabetic WT mice in areas of tubulointerstitial injury, as compared with diabetic SPARC-null mice. We found that the absence of SPARC had a protective effect on tubulointerstitial injury with diminished production of TGF-β1. It has been demonstrated that TGF-β stimulates secretion

of types I and IV collagen by cultured renal interstitial fibroblasts (39). SPARC has been co-localized to cells with a myofibroblastic-like phenotype (*i.e.*, with co-expression of αSMA) in the damaged interstitium in chronic human disease such as chronic transplant rejection (24,30). Given the central role of TGF-β1 in mediating interstitial fibrosis as established in numerous studies of experimental injury (reviewed in reference 40), and the presence of SPARC in relevant sites of tubulointerstitial injury in disease, these findings indicate that the effect of SPARC on TGF-β1 production might be an important pathogenic mechanism in the exacerbation or amelioration of fibrosing renal injury. We recognize that the deficiency of SPARC may exert a beneficial effect in DN by mechanisms not directly involving TGF-β1, but pathways by which this might occur are not yet clearly defined.

In conclusion, we have demonstrated that chronic STZ-induced DN of 24-wk duration was less severe in SPARC-null compared with WT mice. This was evidenced by the reduction in albuminuria, mesangial expansion, and tubulointerstitial injury with decreased production of ECM components, the latter presumably a consequence of reduced production of TGF-β1. This study indicates that SPARC can be an important modulator of glomerulosclerosis and interstitial damage in response to hyperglycemia and might be an attractive target for therapeutic intervention in human diabetic nephropathy.

Acknowledgments

This work was supported in part by the George M. O'Brien Kidney Research Center at the University of Washington (DK 47659) and other individual research grants from the National Institutes of Health (DK 37198, 52121, and 43422; GM 40711; and HL 59475).

References

1. Bornstein P, Sage E: Matricellular proteins: Extracellular modulators of cell function. *Curr Opin Cell Biol* 14: 608, 2002
2. Sasaki T, Hohenester E, Göhring W, Timpl R: Crystal structure and mapping by site-directed mutagenesis of the collagen-binding epitope of an activated form of BM-40/SPARC/osteonectin. *Embo J* 17: 1625–1634, 1998
3. Motamed K, Sage EH: SPARC inhibits endothelial cell adhesion but not proliferation through a tyrosine phosphorylation-dependent pathway. *J Cell Biochem* 70: 543–552, 1998
4. Raines EW, Lane TF, Iruela-Arispe ML, Ross R, Sage EH: The extracellular glycoprotein SPARC interacts with platelet-derived growth factor (PDGF)-AB and -BB and inhibits the binding of PDGF to its receptors. *Proc Natl Acad Sci USA* 89: 1281–1285, 1992
5. Francki A, Bradshaw AD, Bassuk JA, Howe CC, Couser WG, Sage EH: SPARC regulates the expression of collagen type I and transforming growth factor-beta1 in mesangial cells. *J Biol Chem* 274: 32145–32152, 1999
6. Bassuk JA, Pichler R, Rothmier JD, Pippen J, Gordon K, Meek RL, Bradshaw AD, Lombardi D, Strandjord TP, Reed M, Sage EH, Couser WG, Johnson R: Induction of TGF-beta1 by the matricellular protein SPARC in a rat model of glomerulonephritis. *Kidney Int* 57: 117–128, 2000
7. Nomura S, Wills AJ, Edwards DR, Heath JK, Hogan BL: Developmental expression of 2ar (osteopontin) and SPARC (osteonectin) RNA as revealed by in situ hybridization. *J Cell Biol* 106: 441–450, 1988
8. Reed MJ, Puolakkainen P, Lane TF, Dickerson D, Bornstein P, Sage EH: Differential expression of SPARC and thrombospondin 1 in wound repair: Immunolocalization and in situ hybridization. *J Histochem Cytochem* 41: 1467–1477, 1993
9. Shankavaram UT, DeWitt DL, Funk SE, Sage EH, Wahl LM: Regulation of human monocyte matrix metalloproteinases by SPARC. *J Cell Physiol* 173: 327–334, 1997
10. Floege J, Johnson RJ, Alpers CE, Fatemi-Nainie S, Richardson CA, Gordon K, Couser WG: Visceral glomerular epithelial cells can proliferate in vivo and synthesize platelet-derived growth factor B-chain. *Am J Pathol* 142: 637–650, 1993
11. Pichler RH, Bassuk JA, Hugo C, Reed MJ, Eng E, Gordon KL, Pippin J, Alpers CE, Couser WG, Sage EH, Johnson RJ: SPARC is expressed by mesangial cells in experimental mesangial proliferative nephritis and inhibits platelet-derived-growth-factor-medicated mesangial cell proliferation in vitro. *Am J Pathol* 148: 1153–1167, 1996
12. Ibrahim HN, Hostetter TH: Diabetic nephropathy. *J Am Soc Nephrol* 8: 487–493, 1997
13. Border WA, Yamamoto T, Noble NA: Transforming growth factor beta in diabetic nephropathy. *Diabetes Metab Rev* 12: 309–339, 1996
14. Bollineni JS, Reddi AS: Transforming growth factor-beta 1 enhances glomerular collagen synthesis in diabetic rats. *Diabetes* 42: 1673–1677, 1993
15. Kanauchi M, Nishioka M, Dohi K: Secreted protein acidic and rich in cysteine (SPARC) in patients with diabetic nephropathy and tubulointerstitial injury. *Diabetologia* 43: 1076–1077, 2000
16. Gilbert RE, McNally PG, Cox A, Dziadek M, Rumble J, Cooper ME, Jerums G: SPARC gene expression is reduced in early diabetes-related kidney growth. *Kidney Int* 48: 1216–1225, 1995
17. Norose K, Clark JI, Syed NA, Basu A, Heber-Katz E, Sage EH, Howe CC: SPARC deficiency leads to early-onset cataractogenesis. *Invest Ophthalmol Vis Sci* 39: 2674–2680, 1998
18. Bassuk JA, Birkebak T, Rothmier JD, Clark JM, Bradshaw A, Muchowski PJ, Howe CC, Clark JI, Sage EH: Disruption of the Sparc locus in mice alters the differentiation of lenticular epithelial cells and leads to cataract formation. *Exp Eye Res* 68: 321–331, 1999
19. Alpers CE, Hudkins KL, Gown AM, Johnson RJ: Enhanced expression of muscle-specific actin in glomerulonephritis. *Kidney Int* 41: 1134–1142, 1992
20. Ophascharoensuk V, Pippin JW, Gordon KL, Shankland SJ, Couser WG, Johnson RJ: Role of intrinsic renal cells versus infiltrating cells in glomerular crescent formation. *Kidney Int* 54: 416–425, 1998
21. Kamata T, Muso E, Yashiro M, Kawamura T, Oyama A, Matsushima H, Takeuchi E, Yoshida H, Sasayama S: Up-regulation of glomerular extracellular matrix and transforming growth factor-beta expression in RF/J mice. *Kidney Int* 55: 864–876, 1999
22. Taneda S, Segerer S, Hudkins KL, Cui Y, Wen M, Segerer M, Wener MH, Khairallah CG, Farr AG, Alpers CE: Cryoglobulinemic glomerulonephritis in thymic stromal lymphopoietin transgenic mice. *Am J Pathol* 159: 2355–2369, 2001
23. Sage H, Vernon RB, Decker J, Funk S, Iruela-Arispe ML: Distribution of the calcium-binding protein SPARC in tissues of embryonic and adult mice. *J Histochem Cytochem* 37: 819–829, 1989
24. Alpers CE, Hudkins KL, Segerer S, Sage EH, Pichler R, Couser WG, Johnson RJ, Bassuk JH: Localization of SPARC in devel-

oping, mature and injured human kidney. *Kidney Int* 62: 2073–86, 2002
25. Al-Douahji M, Brugarolas J, Brown PA, Stehman-Breen CO, Alpers CE, Shankland SJ: The cyclin kinase inhibitor p21WAF1/CIP1 is required for glomerular hypertrophy in experimental diabetic nephropathy. *Kidney Int* 56: 1691–1699, 1999
26. Pelton RW, Hogan BL, Miller DA, Moses HL: Differential expression of genes encoding TGFs beta 1, beta 2, and beta 3 during murine palate formation. *Dev Biol* 141: 456–460, 1990
27. Alpers CE, Hudkins KL, Ferguson M, Johnson RJ, Rutledge JC: Platelet-derived growth factor A-chain expression in developing and mature human kidneys and in Wilms' tumor. *Kidney Int* 48: 146–154, 1995
28. Floege J, Alpers CE, Sage EH, Pritzl P, Gordon K, Johnson RJ, Couser WG: Markers of complement-dependent and complement-independent glomerular visceral epithelial cell injury in vivo. Expression of antiadhesive proteins and cytoskeletal changes. *Lab Invest* 67: 486–497, 1992
29. Pichler RH, Hugo C, Shankland SJ, Reed MJ, Bassuk JA, Andoh TF, Lombardi DM, Schwartz SM, Bennett WM, Alpers CE, Sage EH, Johnson RJ, Couser WG: SPARC is expressed in renal interstitial fibrosis and in renal vascular injury: *Kidney Int* 50: 1978–1989, 1996
30. Alpers CE, Pichler R, Johnson RJ: Phenotypic features of cortical interstitial cells potentially important in fibrosis. *Kidney Int Suppl* 54: S28–31, 1996
31. Parving H-H, Osterby R, Ritz E: Morphologic features of diabetic nephropathy. In: *The Kidney*, 6th ed, edited by Brenner BM, Philadelphia, W B. Saunders, 2000, pp 1732–1737
32. Tamsma JT, van den Born J, Bruijn JA, Assmann KJ, Weening JJ, Berden JH, Wieslander J, Schrama E, Hermans J, Veerkamp JH, et al: Expression of glomerular extracellular matrix components in human diabetic nephropathy: decrease of heparan sulphate in the glomerular basement membrane. *Diabetologia* 37: 313–320, 1994
33. Suzuki Y: Constituents of the extracellular matrices in diabetic glomerulosclerosis. *Nippon Jinzo Gakkai Shi* 31: 1047–1054, 1989
34. Young BA, Johnson RJ, Alpers CE, Eng E, Gordon K, Floege J, Couser WG, Seidel K: Cellular events in the evolution of experimental diabetic nephropathy. *Kidney Int* 47: 935–944, 1995
35. Yamamoto T, Nakamura T, Noble NA, Ruoslahti E, Border WA: Expression of transforming growth factor beta is elevated in human and experimental diabetic nephropathy. *Proc Natl Acad Sci USA* 90: 1814–1818, 1993
36. Ziyadeh FN, Hoffman BB, Han DC, Iglesias-De La Cruz MC, Hong SW, Isono M, Chen S, McGowan TA, Sharma K: Long-term prevention of renal insufficiency, excess matrix gene expression, and glomerular mesangial matrix expansion by treatment with monoclonal antitransforming growth factor-beta antibody in db/db diabetic mice. *Proc Natl Acad Sci USA* 97: 8015–8020, 2000
37. Ziyadeh FN, Sharma K, Ericksen M, Wolf G: Stimulation of collagen gene expression and protein synthesis in murine mesangial cells by high glucose is mediated by autocrine activation of transforming growth factor-beta. *J Clin Invest* 93: 536–542, 1994
38. Nakamura T, Miller D, Ruoslahti E, Border WA: Production of extracellular matrix by glomerular epithelial cells is regulated by transforming growth factor-beta 1. *Kidney Int* 41: 1213–1221, 1992
39. Alvarez RJ, Sun MJ, Haverty TP, Iozzo RV, Myers JC, Neilson EG: Biosynthetic and proliferative characteristics of tubulointerstitial fibroblasts probed with paracrine cytokines. *Kidney Int* 41: 14–23, 1992
40. Border WA, Noble NA: Transforming growth factor beta in tissue fibrosis. *N Engl J Med* 331: 1286–1292, 1994
41. Kubbutat MH, Key G, Duchrow M, Schluter C, Flad HD, Gerdes J: Epitope analysis of antibodies recognising the cell proliferation associated nuclear antigen previously defined by the antibody Ki-67 (Ki-67 protein). *J Clin Pathol* 47: 524–528, 1994
42. Johnson RJ, Iida H, Alpers CE, Majesky MW, Schwartz SM, Pritzi P, Gordon K, Gown AM: Expression of smooth muscle cell phenotype by rat mesangial cells in immune complex nephritis. Alpha-smooth muscle actin is a marker of mesangial cell proliferation. *J Clin Invest* 87: 847–858, 1991
43. Fouser L, Iruela-Arispe L, Bornstein P, Sage EH: Transcriptional activity of the alpha 1(I)-collagen promoter is correlated with the formation of capillary-like structures by endothelial cells in vitro. *J Biol Chem* 266: 18345–18351, 1991
44. Moiseeva EP, Spring EL, Baron JH, de Bono DP: Galectin 1 modulates attachment, spreading and migration of cultured vascular smooth muscle cells via interactions with cellular receptors and components of extracellular matrix. *J Vasc Res* 36: 47–58, 1999
45. Manthorpe M, Engvall E, Ruoslahti E, Longo FM, Davis GE, Varon S: Laminin promotes neuritic regeneration from cultured peripheral and central neurons. *J Cell Biol* 97: 1882–1890, 1983
46. Rosenberg I, Cherayil BJ, Isselbacher KJ, Pillai S: Mac-2-binding glycoproteins. Putative ligands for a cytosolic beta-galactoside lectin. *J Biol Chem* 266: 18731–18736, 1991